

Electronic Supplementary Information for the Manuscript

The halogen bond made visible: Experimental charge density of a very short intermolecular Cl \cdots Cl donor-acceptor contact.

Ruimin Wang, Thomas Dols, Christian W. Lehmann, and Ulli Englert

Institute of Inorganic Chemistry, RWTH Aachen University, Germany, and
Max-Planck-Institut für Kohlenforschung, Mülheim, Germany

Synthesis:

Chemicals and reagents: Zincchloride and 3,4,5-trichloropyridine and 3-chloro-pyridine were purchased and used without further purification.

Preparation and Crystallization of **1**

Crystals were directly obtained by reactant diffusion: 0.25 mmol (34 mg) ZnCl_2 were dissolved in 5 mL of ethanol and placed in a test tube. 3 mL of EtOH were layer above, and a third layer of 0.5 mmol (91 mg) of trichloropyridine was added. Colourless crystals formed after 3 days. Microanalysis for the solid: C 23.64, H 0.59, N 5.52 %; theoretical for $\text{C}_{10}\text{H}_4\text{N}_2\text{Cl}_8\text{Zn}$: C 23.97, H 0.80, N 5.59%.

Preparation of **2**

10 mmol (1.36 g) of ZnCl_2 and 20 mmol (2.27 g) of 3-chloropyridine were dissolved separately, each in 20 mL of ethanol; the two solutions were mixed and stirred at room temperature. After 20 min, the off-white precipitate was filtered and dried in vacuo. Yield 2.55 g, 70%.

Crystallization of **2**

An excess of **2** was suspended at 50° C in isopropanol; the hot suspension was filtered and the clear filtrate was slowly cooled to room temperature in a warm oil bath. Crystals formed after 15 hrs. Microanalysis for the solid: C 32.86, H 2.19, N 7.80 %; theoretical for $\text{C}_{10}\text{H}_8\text{N}_2\text{Cl}_4\text{Zn}$: C 33.05, H 2.22, N 7.71 %.

Crystallographic studies:

X-ray data collection

Intensity data for **1** were collected at 100 K on a Bruker AXS Mach3 goniometer with Kappa CCD detector. X-rays were generated by a rotating anode (Bruker AXS FR591) using Mo- $K\alpha$ radiation and a graphite monochromator. An Oxford Cryosystems 700 controller was used to ensure temperature stability during data collection.

Intensity data for **2** were collected at 100 K on a Bruker D8 goniometer equipped with an APEX CCD detector using Mo $K\alpha$ radiation ($\lambda = 0.71073 \text{ \AA}$). The radiation source was an

INCOATEC I- μ S microsource equipped with multilayer optics. An Oxford Cryosystems 700 controller was used to ensure temperature stability during data collection.

For both data sets the SAINT software [1] was used for integration. Data were merged with the program SHELXL97.[2] Crystal data and information concerning data collection is compiled in Table S1.

Spherical-atom refinement and multipole refinement

The structures were solved with direct methods and the independent atom refinement was performed by full-matrix least squares on F^2 . [2] Anisotropic displacement parameters were assigned to non-H atoms. Coordinates and isotropic displacement parameters of the only H atom in the asymmetric unit of **1** were refined, whereas the hydrogen atoms in **2** were included in idealized geometry.

The multipolar refinement was based on the independent atom model as starting geometry. It was carried out on F^2 according to the Hansen & Coppens formalism for aspherical atomic density expansion[3] as implemented in *XD2006*. [4] The VM databank was adopted for the refinement. For the metal center, the 12 electrons of $3d^{10}4s^2$ were regarded to populate the valence shell with the initial valence state of +2. Multipole coefficients up to hexadecapoles were refined for non-H atoms. For H atoms, positions were constrained to C-H bond distances of 1.083 Å and monopoles and bond-oriented dipoles were considered in the multipolar refinements. In all refinements the multipoles were introduced stepwise until a full hexadecapole expansion was reached. Convergence results and details about the treatment of contraction parameters have been compiled in Table S2.

1 and **2** are transition metal compounds with suitability factors [5] of 0.35 and 0.43, respectively. Residual densities after the multipole refinement are smaller than after the spherical-atom refinement but still higher than usually encountered for organic compounds; the most prominent maxima and minima are located in the neighborhood of the zinc centers.

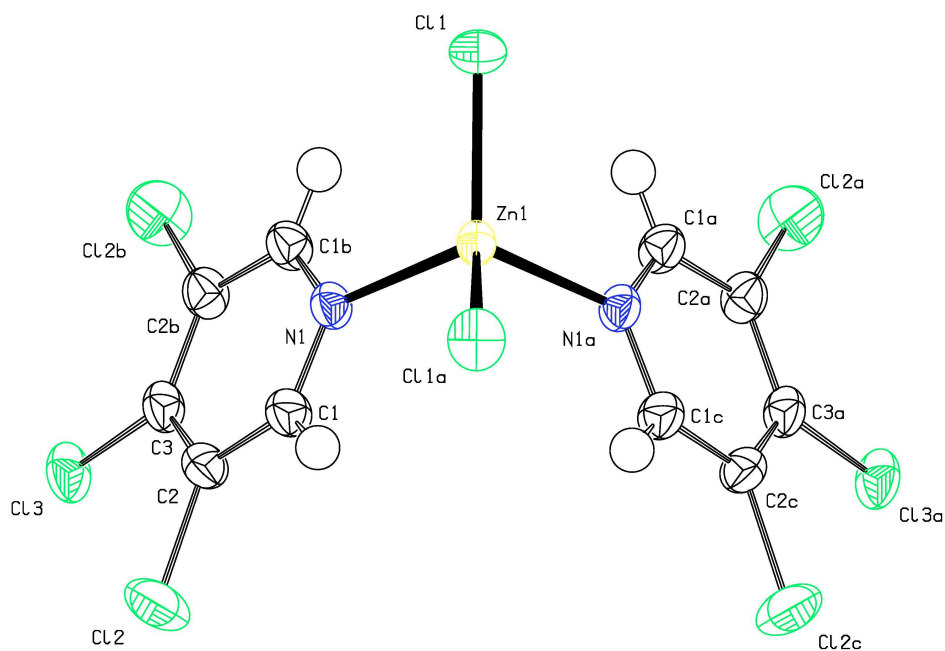


Figure S1. Displacement ellipsoid plots [6] of a complex molecule in **1**, drawn at the 90% probability level. Symmetry operations: a = 1-x, 1-y, z; b = 1-y, 1-x, z; c = y, x, z.

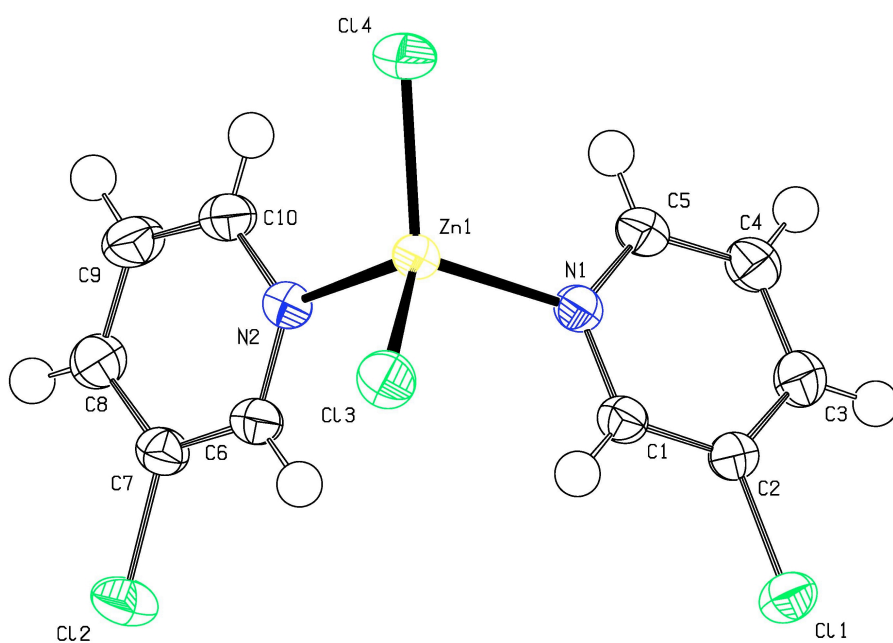


Figure S2. Displacement ellipsoid plots [6] of a complex molecule in **2**, drawn at the 90% probability level.

Table S1 Crystal data and data collection parameters

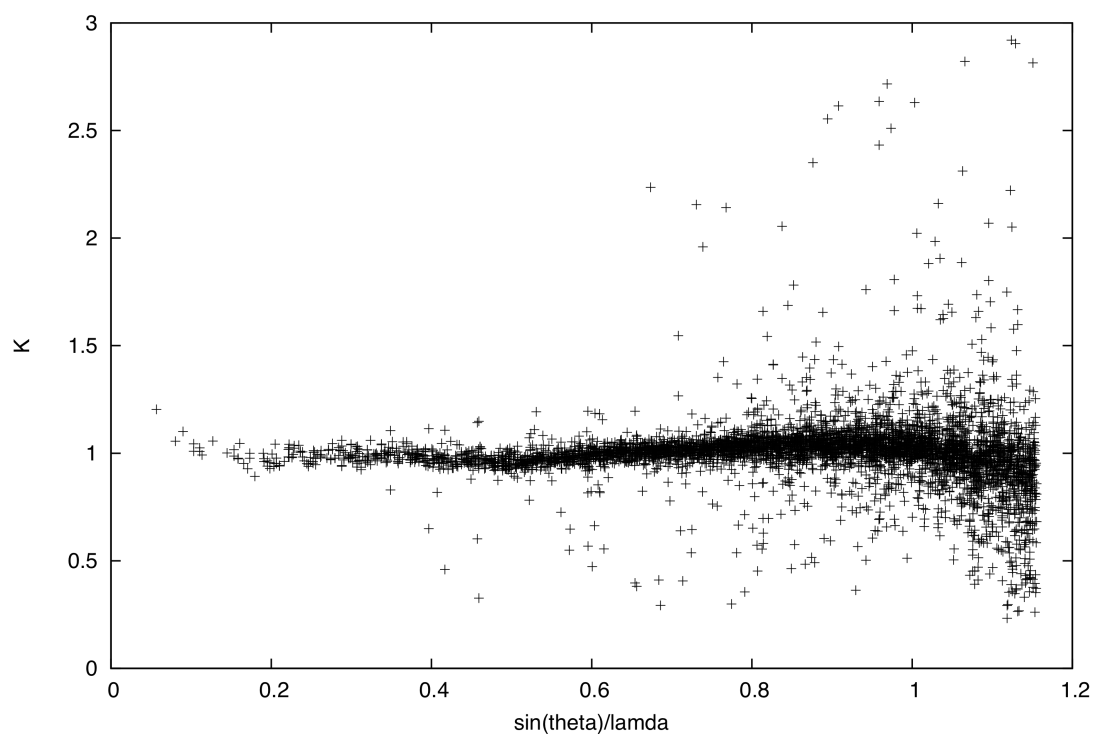
	1	2
Chemical formula	C ₁₀ H ₄ Cl ₈ N ₂ Zn	C ₁₀ H ₈ Cl ₄ N ₂ Zn
M_r	501.12	363.35
Crystal system, space group	Tetragonal, $P4_2nm$	Triclinic, $P-1$
Temperature (K)	100	100
a, b, c (Å)	12.4404(3), 12.4404(3), 5.2602(3)	7.2699(10), 7.8257(11), 13.110(2)
α, β, γ (deg)		84.204(6), 89.280(6), 62.377(5)
V (Å ³)	814.09(5)	656.97(17)
Z	2	2
Radiation type	Mo $K\alpha$	Mo $K\alpha$
μ (mm ⁻¹)	2.811	2.658
Crystal form, size (mm)	Needle, 0.34*0.05*0.03	Prism, 0.29*0.26*0.25
Data collection		
Diffractometer	Bruker Kappa CCD diffractometer (rotating anode)	Bruker <i>APEX</i> CCD diffractometer
Data-collection method	ω scans	ω scans
Absorption correction	Multi-scan <i>SADABS</i>	Multi-scan <i>SADABS</i>
T_{\min}, T_{\max}	0.448, 0.920	0.513, 0.556
$(\sin \theta/\lambda)_{\max}$ (Å ⁻¹)	1.155	1.148
No. of measured, independent, and observed reflections	81346, 5405, 5096	61942, 15656, 12077
Criterion for observed reflections	$I > 2\sigma(I)$	$I > 2\sigma(I)$
R_{int}	0.0426	0.0487
θ_{\max} (°)	55.21	54.71

Table S2 Refinement results on IAM and multipole model

	1	2
IAM model		
Function minimized	F^2	F^2
$R1$ (obs)	0.0268	0.0271
$R1$ (all)	0.0303	0.0363
$wR2$	0.0690	0.0587
a, b in weighting		
scheme	0.02, 0.42	0.02
S	1.051	1.012
$\Delta\rho_{\max}, \Delta\rho_{\min}$ ($\text{e } \text{\AA}^{-3}$)	1.063, -0.744	1.203, -1.090
No. of reflections	5405	15656
No. of parameters	60	154
Flack parameter	0.130(6)	
Multipole model		
Function minimized	F^2	F^2
$R1$ (obs)	0.025	0.022
$R1$ (all)	0.031	0.034
$R2, wR2$	0.035, 0.075	0.038, 0.037
S	1.1399	0.945
$\Delta\rho_{\max}, \Delta\rho_{\min}$ ($\text{e } \text{\AA}^{-3}$)	0.925, -0.584	0.680, -0.803
Contraction		
parameters		
κ	refined for non H atoms; fixed to 1.13 for H	refined for non H atoms; fixed to 1.13 for H
κ'	fixed to 1.2 for Zn, Cl, H refined for N, C	fixed to 1.0 for Cl, 1.2 for H refined for other atom types

Data quality and completeness for intensity data of **1**

Plot of ratio K vs $\sin\theta/\lambda$; K is the ratio $F^2_{\text{obs}}/F^2_{\text{calc}}$



Summary of completeness for the experimental charge density data (Friedel pairs merged!)

θ	$\sin(\theta_{\text{max}})/\lambda$	Complete	*Expected	*Measured	*Missing	*cumulative
20.82	0.500	0.993	268	266	2	
23.01	0.550	0.994	344	342	2	
25.24	0.600	0.995	443	441	2	
----- ACTA Min. Res. ----						
27.51	0.650	0.996	551	549	2	
29.84	0.700	0.997	686	684	2	
32.21	0.750	0.998	836	834	2	
34.65	0.800	0.998	1002	1000	2	
37.17	0.850	0.998	1188	1186	2	
39.77	0.900	0.999	1406	1404	2	
42.47	0.950	0.999	1636	1634	2	
45.29	1.000	0.999	1905	1903	2	
48.27	1.050	0.999	2190	2188	2	
51.43	1.100	0.999	2513	2511	2	
54.82	1.150	0.999	2853	2851	2	
55.21	1.156	0.997	2904	2895	9	

Summary of completeness for the experimental charge density data (Friedel pairs unmerged!)

overall SMAX = $\sin(\theta_{\max})/\lambda = 1.156 \text{ \AA}^{-1}$

overall DMIN = $1/(2*\sin(\theta_{\max})/\lambda) = 0.43 \text{ \AA}$

N = 5682 MEASURED UNIQUE HKL

M = 74 MISSING UNIQUE HKL WITH $\sin(\theta_{\max})/\lambda < \text{SMAX}$

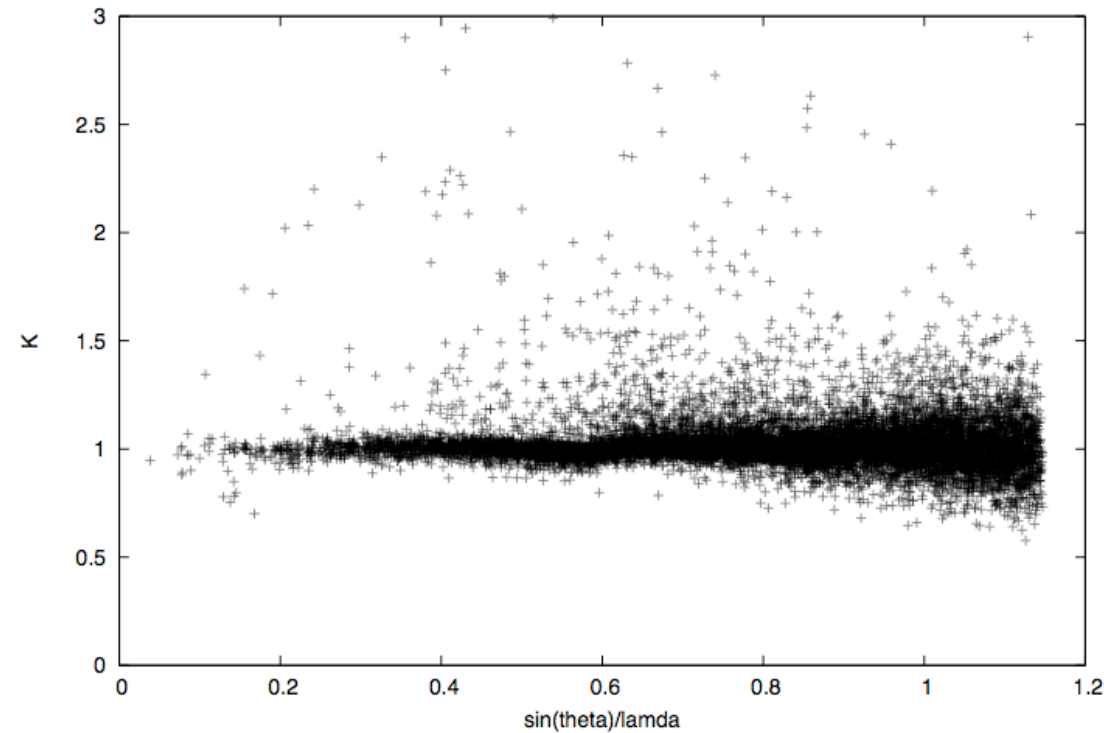
overall completeness = 98.7%

DISTRIBUTION OF MEASURED AND MISSING REFLECTIONS IN EQUAL-VOLUME RESOLUTION SHELLS

SHELL SMAX	SHELL DMIN	NHKL MEASURED	NHKL MISSING	PERCENT COMPLETENESS
0.4257	1.175	324	9	97.3
0.5363	0.932	300	1	99.7
0.6140	0.814	287	5	98.3
0.6758	0.740	280	7	97.6
0.7279	0.687	294	5	98.3
0.7736	0.646	271	5	98.2
0.8143	0.614	294	5	98.3
0.8514	0.587	269	2	99.3
0.8855	0.565	283	4	98.6
0.9171	0.545	287	2	99.3
0.9468	0.528	273	2	99.3
0.9746	0.513	287	2	99.3
1.0010	0.500	280	0	100.0
1.0260	0.487	291	2	99.3
1.0499	0.476	261	1	99.6
1.0727	0.466	283	1	99.6
1.0946	0.457	283	0	100.0
1.1157	0.448	284	0	100.0
1.1359	0.440	267	1	99.6
1.1555	0.433	284	21	93.1

Data quality and completeness for intensity data of **2**

Plot of ratio K vs $\sin\theta/\lambda$; K is the ratio $F^2_{\text{obs}}/F^2_{\text{calc}}$



Summary of completeness for the experimental charge density data

θ	$\sin(\theta_{\text{max}})/\lambda$	Complete	*Expected	*Measured	*Missing	*cumulative
20.82	0.500	1.000	1369	1369	0	
23.01	0.550	1.000	1833	1833	0	
25.24	0.600	1.000	2389	2389	0	
----- ACTA Min. Res. ---						
27.51	0.650	1.000	3022	3022	0	
29.84	0.700	0.999	3760	3756	4	
32.21	0.750	0.998	4635	4625	10	
34.65	0.800	0.996	5656	5633	23	
37.17	0.850	0.994	6755	6712	43	
39.77	0.900	0.991	8003	7933	70	
42.47	0.950	0.988	9434	9317	117	
45.29	1.000	0.983	11014	10830	184	
48.27	1.050	0.975	12755	12432	323	
51.43	1.100	0.964	14631	14110	521	
54.71	1.148	0.940	16656	15656	1000	

Table S3. Topological properties for bond critical points in **1**; dist is the interatomic distance, d_{ij} the total bond path $d_1 + d_2$, d_1 and d_2 the distances from the bond critical point to the 1st and 2nd atom along the bond path; ρ and $\nabla^2\rho$ represent the electron density and its Laplacian at the bond critical point. Note the large discrepancy between the interatomic distance $H(1) \cdots Cl(3)^b$ and the bond path due to the pronounced curvature of the latter.

Bond	dist (Å)	d_{ij} (Å)	d_1 (Å)	d_2 (Å)	ρ (eÅ ⁻³)	∇^2 (eÅ ⁻⁵)
Cl(1)···Cl(3) ^a	3.1912(6)	3.1912	1.5779	1.6133	0.107(2)	1.102(4)
H(1) ···Cl(3) ^b	2.84	3.0412	1.2529	1.7882	0.054(6)	0.424(3)
Zn(1)–Cl(1)	2.2048(3)	2.2051	1.0161	1.1890	0.47(2)	5.03(2)
Zn(1)–N(1)	2.0764(8)	2.0798	1.0320	1.0478	0.38(2)	7.12(3)
Cl(2)–C(2)	1.7113(7)	1.7118	0.9425	0.7694	1.41(8)	–7.1(2)
Cl(3)–C(3)	1.7014(9)	1.7144	1.0042	0.7102	1.53(5)	–13.1(2)
N(1)–C(1)	1.3379(8)	1.3437	0.8686	0.4752	2.41(7)	–36.7(3)
C(3)–C(2)	1.3980(8)	1.3984	0.7366	0.6618	2.31(6)	–27.3(2)
C(2)–C(1)	1.3882(10)	1.3900	0.6755	0.7146	2.16(6)	–28.4(2)
C(1)–H(1)	1.083	1.0850	0.6618	0.4232	1.7(2)	–13.9(4)

a= 3/2–y, 1/2+x, 3/2+z

b= –1/2+y, 1/2–x, 1/2+z

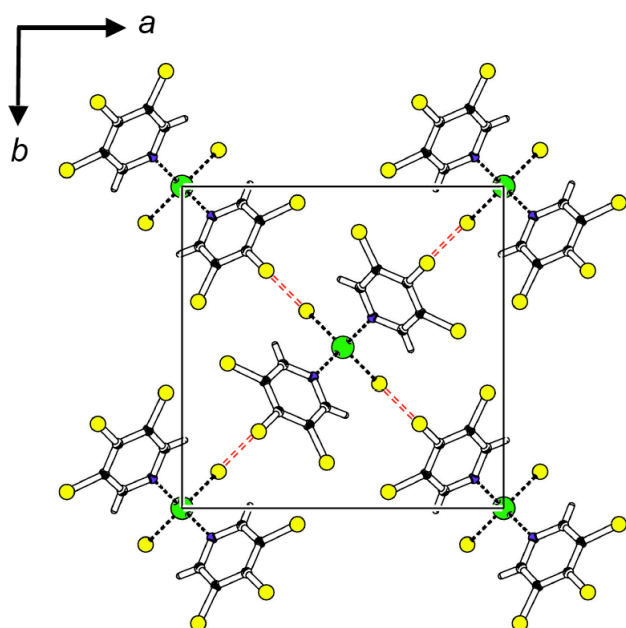


Figure S3. Packing diagram [6] for **1**; the short Cl...Cl contacts are shown as dashed red lines.

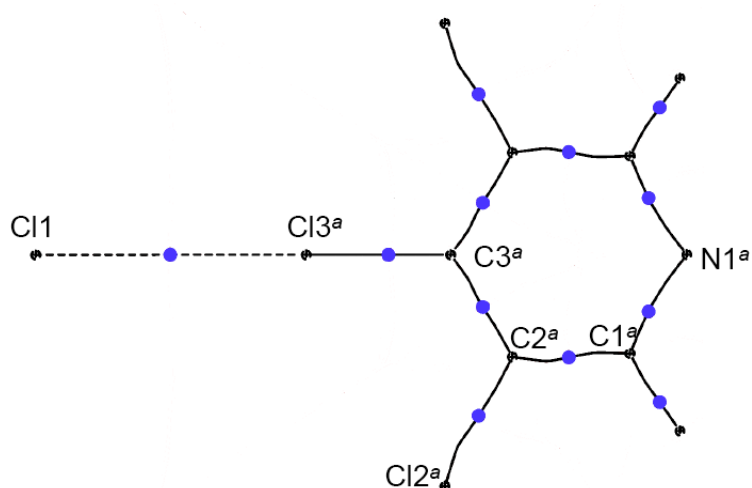


Figure S4. Molecular graph [4] around the short Cl...Cl contacts in **1**; nuclear attractors and bond paths are shown in black (Cl...Cl dashed), bond critical points in blue.

Table S4. Topological properties for bond critical points in **2**; dist is the interatomic distance, d_{ij} the total bond path $d_1 + d_2$, d_1 and d_2 the distances from the bond critical point to the 1st and 2nd atom along the bond path; ρ and $\nabla^2\rho$ represent the electron density and its Laplacian at the bond critical point.

Bond	dist(Å)	d _{ij} (Å)	d ₁ (Å)	d ₂ (Å)	ρ(eÅ ⁻³)	∇2(eÅ ⁻⁵)
Cl(1)···Cl(1) ^a	3.3651(6)	3.3650	1.6825	1.6825	0.048(2)	0.576(2)
Cl(2)···Cl(2) ^b	3.5480(6)	3.5480	1.7738	1.7742	0.041(2)	0.489(2)
Cl(1)···H(3) ^c	2.77	2.7684	1.7466	1.0218	0.046(7)	0.632(2)
Cl(4)···H(10)	2.73	2.7416	1.6335	1.1081	0.080(3)	0.841(2)
Zn(1)–Cl(3)	2.22445(14)	2.2246	1.0359	1.1887	0.437(7)	6.855(4)
Zn(1)–Cl(4)	2.21662(14)	2.2171	1.0336	1.1835	0.387(7)	6.403(4)
Zn(1)–N(1)	2.0514(6)	2.0534	1.0011	1.0523	0.532(8)	8.89(2)
Zn(1)–N(2)	2.0831(6)	2.0834	1.0133	1.0701	0.509(8)	8.88(2)
Cl(1)–C(2)	1.7218(5)	1.7226	0.9784	0.7442	1.37(2)	–4.20(5)
Cl(2)–C(7)	1.7199(5)	1.7208	0.9203	0.8004	1.20(2)	–0.11(5)
N(1)–C(1)	1.3453(7)	1.3457	0.8255	0.5202	2.45(3)	–27.6(2)
N(1)–C(5)	1.3475(6)	1.3495	0.7698	0.5797	2.29(3)	–23.23(9)
N(2)–C(6)	1.3434(7)	1.3447	0.7945	0.5503	2.29(3)	–21.9(2)
N(2)–C(10)	1.3443(7)	1.3443	0.8239	0.5205	2.53(3)	–33.1(2)
C(1)–C(2)	1.3869(7)	1.3869	0.6878	0.6991	2.20(2)	–21.95(6)
C(1)–H(1)	1.083	1.0833	0.7797	0.3036	1.72(4)	–18.3(2)
C(2)–C(3)	1.3930(7)	1.3936	0.7824	0.6113	1.93(3)	–17.05(8)
C(3)–C(4)	1.3898(8)	1.3897	0.6782	0.7115	2.07(2)	–19.83(6)
C(3)–H(3)	1.083	1.0842	0.7629	0.3213	1.83(5)	–19.9(2)
C(4)–C(5)	1.3886(7)	1.3893	0.7131	0.6762	2.17(2)	–20.9(2)
C(4)–H(4)	1.083	1.0842	0.7595	0.3247	1.66(4)	–15.3(2)
C(5)–H(5)	1.083	1.0858	0.7903	0.2955	1.70(5)	–14.5(2)
C(6)–C(7)	1.3918(7)	1.3926	0.5976	0.7950	2.21(2)	–21.72(9)
C(6)–H(6)	1.083	1.0834	0.7876	0.2958	1.79(5)	–20.3(2)
C(7)–C(8)	1.3874(8)	1.3873	0.6707	0.7167	2.36(2)	–25.39(6)
C(8)–C(9)	1.3890(8)	1.3892	0.7064	0.6828	2.17(2)	–20.09(6)
C(8)–H(8)	1.083	1.0834	0.7896	0.2938	1.65(5)	–16.2(3)
C(9)–C(10)	1.3887(8)	1.3894	0.7371	0.6524	2.23(2)	–22.79(7)
C(9)–H(9)	1.083	1.0845	0.8056	0.2790	1.71(5)	–19.4(3)
C(10)–H(10)	1.083	1.0875	0.7819	0.3056	1.84(5)	–19.0(2)
a=–1–x,–y,1–z						
b=–1–x,1–y,–z						
c=–x,–1–y,1–z						

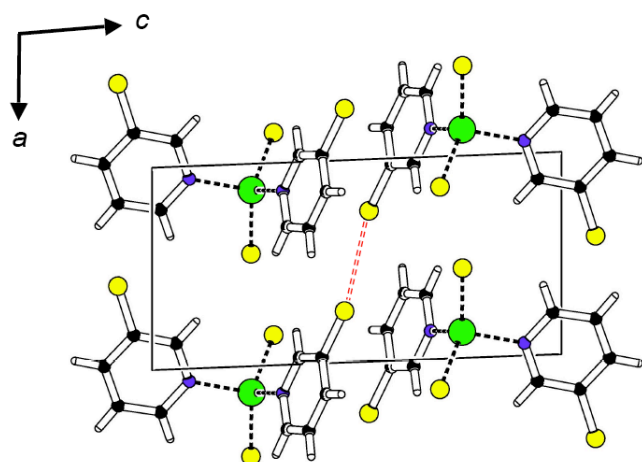


Figure S5. Packing diagram [6] for **2**; the short Cl...Cl contacts are shown as dashed red lines.

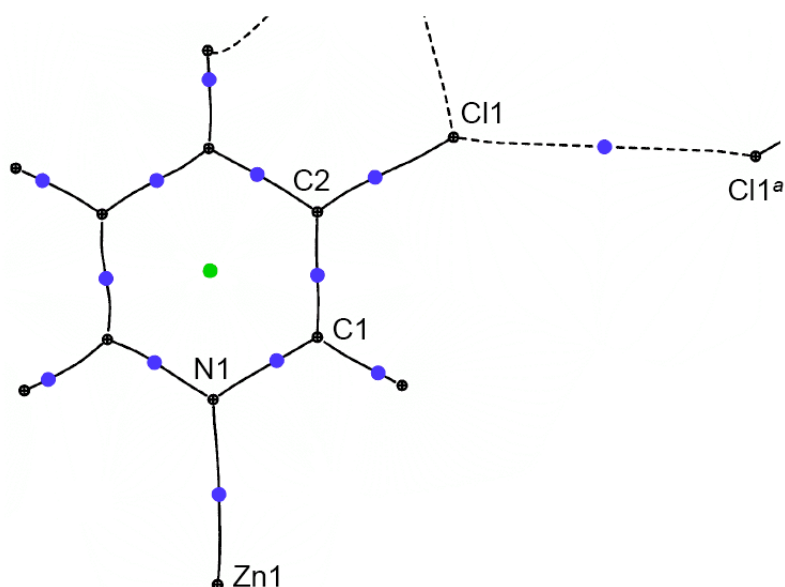


Figure S6. Molecular graph [4] around the short Cl...Cl contacts in **2**; nuclear attractors and bond paths are shown in black (Cl...Cl and hydrogen bonds dashed), bond critical points in blue, ring critical point in green.

References:

1. Bruker SAINT, Version 6.45. Bruker AXS Inc., Madison, Wisconsin, USA, **2003**.
2. Sheldrick, G. M. *Acta Crystallogr. Sect A* **2008**, 64, 112.
3. Hansen, N. K. & Coppens, P. *Acta Crystallogr. Sect A* **1978**, 34, 909.
4. Volkov, A., Macchi, P., Farrugia, L. J., Gatti, C., Mallison, P. R., Richter, T. & Koritsanszky, T. XD2006, University of New York at Buffalo, USA, **2006**.
5. Coppens, P. *Isr. J. Chem.* **1977**, 16, 144–148.
6. Spek, A. L. *Acta Crystallogr. Sect. D*, **2009**, 65, 148.